



Design of Triple-Band Bandpass Filter Using Cascade Tri-Section Stepped Impedance Resonators

Gunawan Wibisono^{1,*}, Teguh Firmansyah² & Tierta Syafraditya¹

^{1,3}Department of Electrical Engineering, Faculty of Engineering Universitas Indonesia
Kampus Baru UI Depok, 16424, Indonesia

²Departement of Electrical Engineering, University of Sultan Agung Tirtayasa
Kampus Cilegon, 42435, Banten, Indonesia

*E-mail: gunawan@eng.ui.ac.id

Abstract. In this research, a triple-band bandpass filter (BPF) using a cascade tri section step impedance resonator (TSSIR), which can be operated at 900 MHz, 1,800 MHz, and 2,600 MHz simultaneously, was designed, fabricated and evaluated. Advanced Design System (ADS) was used to design and simulate the proposed BPF. The proposed BPF using cascade TSSIR was fabricated on an FR4 substrate with dielectric permittivity, substrate thickness and loss tangent at 4.3, 1.6 mm and 0.0017, respectively. The performance parameters of the proposed BPF were characterized by insertion loss, return loss, voltage standing wave ratio (VSWR) and group delay. The performance results from the simulation were compared to those of the fabricated BPF. The results showed that the performances from both the simulated and the fabricated BPF satisfied the design specifications and were in close agreement with each other. Furthermore, the results indicated that the proposed BPF using cascade TSSIR performed better than a hairpin BPF with TSSIR.

Keywords: *cascade TSSIR; group delay; hairpin BPF; insertion and return losses; Triple-band BPF; VSWR.*

1 Introduction

The rapid progress in mobile and wireless technology has increased the need of integrating more than one communication standard or technology into a single system [1-11] where different standards may operate in different frequency bands. Multiband radio frequency (RF) and microwave modules play an important role in a variety of modern communication systems. The microwave multiband bandpass filter (BPF) is one of the most important modules in the front-end circuit. Conventionally, in designing a multiband BPF, the principle of stepped impedance resonators (SIRs) is often used as a building block, due to their multiband behavior, simple structure and well-established design methodology [2-4]. However, the resonance frequencies of the SIRs are dependent on each other, the filter design is quite complicated and it is not convenient to meet specific bandwidth (BW) requirements.

To construct a triple-band microwave BPF, usually two or more SIRs of different resonance frequencies are needed due to the dependence of the third resonance frequency on the first two SIRs [5]. This method results in a large circuit and a complex BPF configuration. To reduce the circuit size and to add design flexibility, a tri-section SIR (TSSIR) with tunable first three resonance frequencies was proposed by Zang, *et al.* [7]. It was indicated in Packiaraj, *et al.* [8] that under the same demanded filter specifications, the electric length of a TSSIR can be designed shorter than that of a two-section SIR.

Triple-band TSSIR BPFs using a hairpin structure were designed and evaluated by Chu, *et al.* [1], Eroglu, *et al.* [2] and Wibisono, *et al.* [10]. However, the triple-band TSSIR using a hairpin structure has a stop-band rejection characteristic that does not satisfy the requirements and the BW of the first band has a narrow band [10]. This is due to the fact that the coupling of the filter happens only at one resonator; otherwise, the input/output port is connected to the third resonator, hence the BW of the first band is narrow.

In this research, a triple-band BPF using cascade TSSIR was designed, fabricated and analyzed. The cascade TSSIR BPF is proposed as an enhancement of the conventional TSSIR [5] in order to improve the stopband rejection response of the hairpin TSSIR [10]. Implementation of the cascade TSSIR is done using two TSSIRs that are coupled to each other in the third resonator. The structure is designed to get transmission zero response at the third band. Thus, the stopband response is improved. To get a wider BW and improve the first frequency response, the input and output ports are connected to the first resonator. The performance parameters of the proposed BPF were characterized by insertion loss (S_{21}), return loss (S_{11}), voltage standing wave ratio (VSWR) and group delay. The performance results from the simulation were compared to those of the fabricated BPF.

The design and research methodology are detailed in the following sections. Section 2 describes the design of the proposed BPF using cascade TSSIR. Results and discussion of the performance test of the fabricated BPF are reported in Section 3. Finally, Section 4 concludes this paper.

2 Triple-Band BPF Design

To design a triple-band BPF, a TSSIR as an enhancement of the SIR was used. The TSSIR structure to be considered is shown in Figure 1 of [1], where the TSSIR has three different impedance characteristics: Z_1 , Z_2 , and Z_3 . For practical application this is preferable to having an equal electrical length. Then, the condition for the fundamental resonance of the TSSIR can be derived as reported in Chu, *et al.* [1], Eroglu, *et al.* [2] and Lin, *et al.* [5].

$$\theta = \tan^{-1} \sqrt{\frac{K_1 K_2}{K_1 + K_2 + 1}} \quad (1)$$

where K_1 and K_2 are the ratios of the impedance resonators represented by $K_1 = Z_3/Z_2$ and $K_2 = Z_2/Z_1$, respectively.

The total electrical length of the resonator at the fundamental resonance, θ_T , is given by Chu, *et al.* [1], Eroglu, *et al.* [2] and Lin, *et al.* [5]:

$$\theta_T = 6\theta = 6 \tan^{-1} \sqrt{\frac{K_1 K_2}{K_1 + K_2 + 1}} \quad (2)$$

The first spurious passband, “ f_{s1} ” (second passband), occurs at

$$f_{s1} = \frac{\theta_{s1}}{\theta} f_0 \quad (3)$$

where

$$\theta_{s1} = \tan^{-1} \sqrt{\frac{1 + K_1 + K_1 K_2}{K_2}} \quad (4)$$

and, f_0 is the zero spurious passband. The second spurious passband, “ f_{s2} ” (third passband), occurs at

$$f_{s2} = \frac{\theta_{s2}}{\theta} f_0 \quad (5)$$

where

$$\theta_{s2} = \frac{\pi}{2} \quad (6)$$

From Eqs. (1), (3), and (4) we can obtain the first frequency ratio as expressed in Chu, *et al.* [1], Eroglu, *et al.* [2] and Lin, *et al.* [5]:

$$\frac{f_{s1}}{f_0} = \frac{\theta_{s1}}{\theta} = \frac{\tan^{-1} \sqrt{\frac{1 + K_1 + K_1 K_2}{K_2}}}{\tan^{-1} \sqrt{\frac{K_1 K_2}{K_1 + K_2 + 1}}} \quad (7)$$

From Eqs. (1), (5) and (6) another frequency ratio can be expressed as in [1,5]:

$$\frac{f_{s2}}{f_0} = \frac{\theta_{s2}}{\theta} = \frac{\pi}{\tan^{-1} \sqrt{\frac{K_1 K_2}{K_1 + K_2 + 1}}} \quad (8)$$

By properly determining the impedance ratios of K_1 and K_2 , three passbands with any desired frequency ratio can be obtained. The impedance ratios K_1 and K_2 can be derived according to the three desired frequencies f_0 , f_{s1} , and f_{s2} of the passbands from Eqs. (7) and (8) as in [1,5]:

$$\begin{cases} K_1 = \frac{-\cos \alpha \cos \beta + \sqrt{\cos^2 \alpha \cos^2 \beta + 4 \sin^2 s \cos^2(rs)}}{2 \cos^2(rs)} \\ K_2 = \frac{1+K_1}{\tan^2(rs)-K_1} \end{cases} \quad (9)$$

where

$$r = \frac{f_{s1}}{f_0}, \quad s = \frac{\pi f_0}{2 f_{s2}}, \quad \alpha = \frac{\pi f_{s1} + f_0}{2 f_{s2}}, \quad \beta = \frac{\pi f_{s1} - f_0}{2 f_{s2}}$$

By determining the impedance ratios of K_1 and K_2 , three different characteristic impedances, i.e. Z_1 , Z_2 , and Z_3 , can be obtained, where the characteristic impedance Z_C is given by Hong, *et al.* [11]:

$$Z_c = \frac{60}{\sqrt{\epsilon_{re}}} \ln \left[\frac{F}{W/h} + \sqrt{1 + \left(\frac{2}{W/h} \right)^2} \right] \quad (10)$$

where

$$F = 6 + (2\pi - 6) \exp \left[- \left(\frac{30.666}{W/h} \right)^{0.7528} \right]$$

The effective dielectric constant (ϵ_{re}) is given by Hong, *et al.* [11]:

$$\epsilon_{re} = \frac{\epsilon_r + 1}{2} + \frac{\epsilon_r - 1}{2} \left(1 + \frac{10}{W/h} \right)^{xy} \quad (11)$$

where

$$x = 1 + \frac{1}{49} \ln \left(\frac{(W/h)^4 + \left(\frac{W/h}{52} \right)^2}{(W/h)^4 + 0.432} \right) + \frac{1}{18.7} \ln \left[1 + \left(\frac{(W/h)}{18.1} \right)^2 \right]$$

and

$$y = 0.564 \left(\frac{\epsilon_r - 0.9}{\epsilon_r + 3} \right) 0.053$$

W is microstrip width and h is dielectric material thickness. The ratio of W/h is given by Hong, *et al.* [11]:

$$\frac{W}{h} = \begin{cases} \frac{8 \exp(A)}{\exp(2A) - 2} & W/h \leq 2 \\ \frac{\pi}{2} \left\{ (B - 1) - \ln(2B - 1) + \frac{\epsilon_r - 1}{\epsilon_r + 1} \left[\ln(2B - 1) + 0.39 - \frac{0.61}{\epsilon_r} \right] \right\} & W/h \geq 2 \end{cases} \quad (12)$$

where

$$A = \frac{Z_c}{60} \left\{ \frac{\epsilon_r + 1}{2} \right\} 0.5 + \frac{\epsilon_r}{\epsilon_r} \left(0.23 + \frac{0.11}{\epsilon_r} \right)$$

$$B = \frac{60\pi z}{z_c \sqrt{\epsilon_r}}$$

The cascade TSSIR BPF is proposed as an enhancement of the TSSIR in order to improve the stopband rejection response of the triple band hairpin TSSIR from Wibisono, *et al.* [10]. The specifications of the proposed triple-band BPF using cascade TSSIR are the same as for the hairpin BPF in Wibisono, *et al.* [10], as shown in Table 1.

Table 1 Specifications of proposed triple-band BPF using cascade TSSIR.

Center Frequency (MHz)	950	1,850	2,650
BW (MHz)	100	100	100
Insertion Loss, S_{21} (dB)	> -3	> -3	> -3
Return Loss, S_{11} (dB)	< -10	< -10	< -10
VSWR	< 2	< 2	< 2

The structure of the proposed triple-band BPF using cascade TSSIR is shown in Figure 1. The proposed BPF using cascade TSSIR was constructed from two identical TSSIRs, which were coupled at the third resonator in order to achieve better stopband performance. To improve the BW value, the input/output port was connected at the first resonator. The proposed BPF using cascade TSSIR was designed to improve the performance of the hairpin BPF using TSSIR [10] and to minimize the hairpin structure. The dimensions of the proposed BPF using cascade TSSIR were obtained using the method employed in Lin, *et al.* [5] and Wibisono, *et al.* [10].

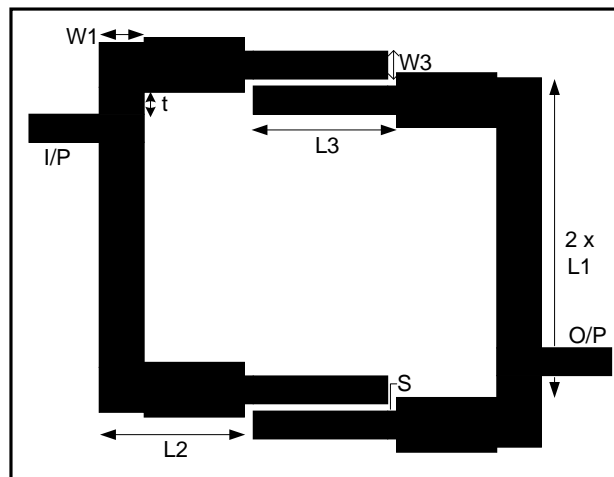


Figure 1 Layout of triple band BPF with cascade TSSIR.

The calculated dimensions of the proposed BPF using cascaded TSSIR were obtained using Eqs. (1)-(12). For comparison, the optimized dimensions of the proposed BPF using cascade TSSIR simulated using ADS are shown in Table 2. The optimized dimensions were simulated in order to find the fixed three frequency centers that can be operated by the proposed BPF. The calculated dimensions were close to the optimized dimensions. The total size of the proposed BPF was $5.4 \times 7.03 \text{ cm}^2$, which is smaller than the size of the hairpin BPF in Wibisono, *et al.* [10].

Table 2 Comparison of dimensions of cascade TSSIR from calculation and optimized ADS.

Dimension	Size (mm)	
	Calculated	Optimized
W1	4.8596	5
W2	5.0473	6.1
W3	3.1118	3.1118
L1	15.3507	15.3507
L2	15.3238	16.2
L3	15.6568	16

3 Simulation Results

The performance of the proposed BPF using cascade TSSIR was characterized by return loss (S_{11}), insertion loss (S_{21}), VSWR, and group delay. S_{11} expresses the input reflection coefficient to show the effectiveness of the BPF in transmitting the signal from the generator to the load. Meanwhile, S_{21} and VSWR were simulated to see if the proposed BPF will transmit all power from input to the output of the filter and not cause mismatch to the load, respectively. Group delay was simulated to show phase shift and distortion when the signal passes to the BPF.

Figure 2 shows the simulation results of S_{11} and S_{21} of the proposed BPF using cascade TSSIR. It can be seen from Figure 2 that the simulation results of S_{11} and S_{21} with center frequency at 950 MHz were -38.434 dB and -0.123 dB, respectively. The BW at a center frequency of 950 MHz was 107 MHz, or fractional BW (FBW) = 11.26 %. Here, FBW denotes the ratio between BW and center frequency. At a center frequency of 1,850 MHz, $S_{11} = -40.426$ dB, $S_{21} = -0.161$ dB, and BW = 299 MHz or FBW = 16.16 %. At a center frequency of 2,650 MHz, $S_{11} = -41.196$ dB, $S_{21} = -0.135$ dB, and BW = 425 MHz or FBW = 16.03%.

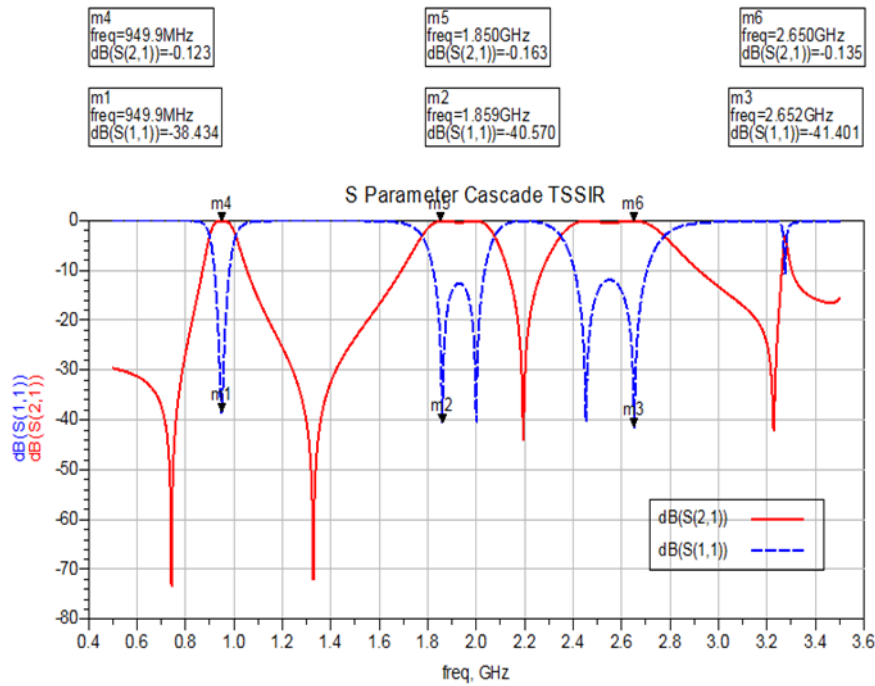


Figure 2 The S11 and S21 results of the simulated BPF using cascade TSSIR.

It can be seen from Figure 2 that the simulation results of S_{11} and S_{21} satisfied the design specifications, while BW performance was achieved only at the center frequency of 950 MHz. The results showed that S_{11} performance was < -10 dB. This means that the proposed BPF can transfer all power from input to output of the BPF; there was no reflection signal back to the input BPF. The input impedances of the proposed BPF were $Z_0^*(1.019 - j0.094)$ at a center frequency of 950 MHz, $Z_0^*(1.092 + j 0.040)$ at a center frequency of 1,850 MHz, and $Z_0^*(0.983 - j0.144)$ at a center frequency of 2,650 MHz, respectively, where Z_0 is the impedance characteristic. These input impedances indicate that the reflection signal back to the input BPF was very small (near to zero). This is also because the cascade construction was successful in getting transmission zero response at the third band. Thus, the stopband response was improved, indicated by the very small value of S_{11} . It can be concluded that the proposed BPF matched the transmission line input and can operate properly at three different frequencies simultaneously.

The S_{21} performance values were near to 0 dB, which means that the proposed BPF can transmit all the power to the load and dissipates less power at the BPF. It can be concluded that the proposed BPF using cascade TSSIR can be

operated well at center frequencies of 950 MHz, 1,850 MHz and 2,650 MHz simultaneously.

Figure 3 shows the VSWR simulation results of the proposed BPF using cascade TSSIR. It can be seen from Figure 3 that the VSWRs of the proposed BPF were 1.024, 1.158 and 1.029 at center frequencies of 950MHz, 1,850 MHz and 2,650 MHz, respectively. All three VSWRs were in close agreement with the design requirements. It was found that the S_{21} performances of the proposed BPF had value > -2 dB, which indicates that all signals were passed by the BPF at three frequencies simultaneously. This is because the proposed BPF has input and output impedances that match each other. Therefore, the VSWR values of the proposed BPF were close to 1.00 and the proposed BPF can be operated well at three frequencies simultaneously.

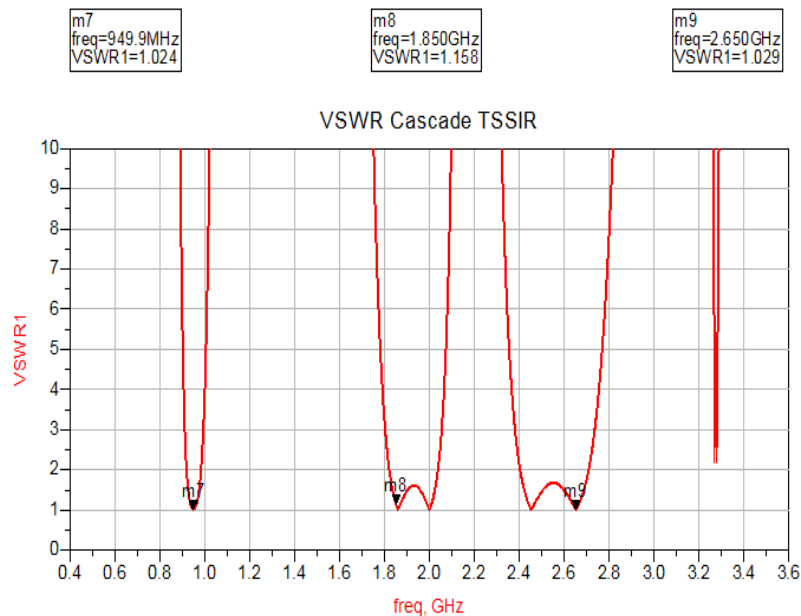


Figure 3 The VSWR results of the simulated BPF using cascade TSSIR.

Figure 4 shows the simulation results of the group delay of the proposed BPF using cascade TSSIR. It can be seen from Figure 4 that the group delay results were 3.67, 1.47 and 0.83 ns at center frequencies of 950 MHz, 1,850 MHz, and 2,650 MHz, respectively. All three group delays were in close agreement with the design requirement. This indicates that the proposed BPF can operate well at three frequencies simultaneously, not causing significant phase shift and distortion when the signal passes to the filter. This occurs because the proposed

BPF has good S_{21} and VSWR performances, so there was no significant distortion as indicated by group delay < 10 ns. It can be concluded that the proposed BPF using cascade TSSIR can be operated well at three frequencies simultaneously.

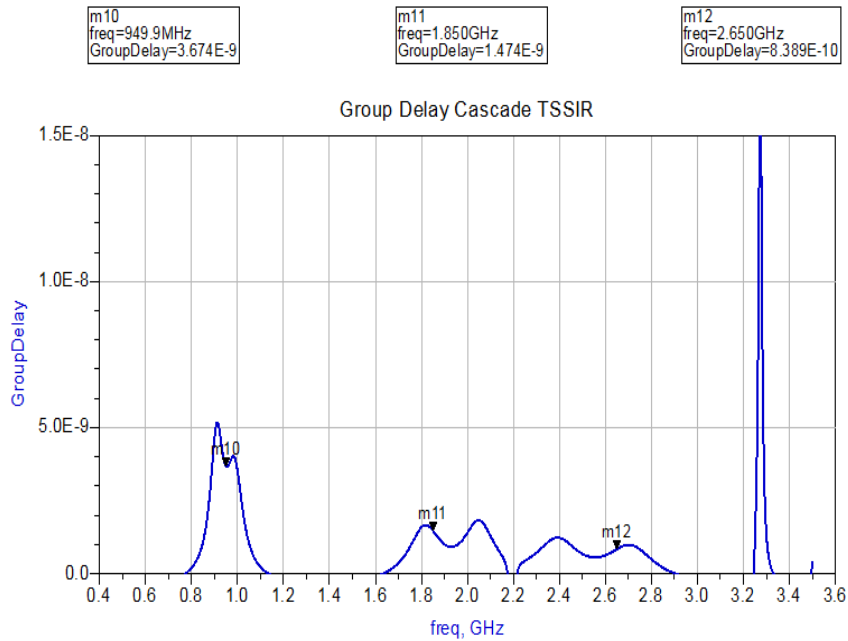


Figure 4 The group delay results of the simulated BPF using cascade TSSIR.

Table 3 Performance results of simulated results of proposed BPF using cascade TSSIR.

Parameters	BPF Using Cascade TSSIR		
Center Frequency (MHz)	950	1,850	2,650
S_{21} (dB)	- 0.12	- 0.16	- 0.14
S_{11} (dB)	- 38.43	- 40.57	- 41.40
VSWR	1.02	1.16	1.03
BW (MHz)	107	299	425
FBW (%)	11.26	16.16	16.03

A summary of the performance results of the proposed BPF using cascade TSSIR is shown in Table 3. It can be seen from Table 3 that the performance results of the proposed BPF satisfy the requirement performances as given in Table 1.

4 Fabricated BPF Results

The proposed BPF using cascade TSSIR was fabricated on FR4 substrate with dielectric permittivity, substrate thickness and loss tangent at 4.3, 1.6 mm and 0.0017, respectively. Figure 5 shows the fabricated version of the proposed BPF using cascade TSSIR. The three passbands of the proposed BPF using cascade TSSIR were located at center frequencies of 950 MHz, 1,850 MHz, and 2,650 MHz. The fabricated BPF using cascade TSSIR had smaller dimensions than those of the hairpin BPF using TSSIR as proposed in [10].

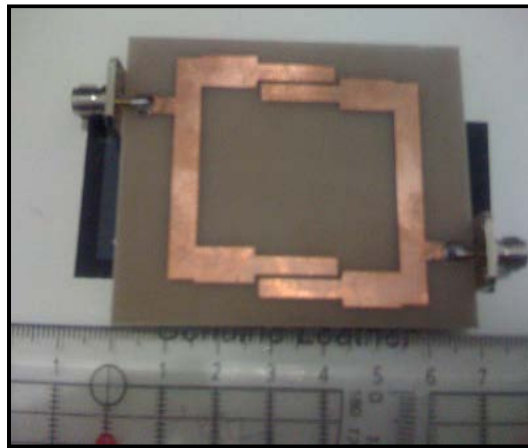


Figure 5 The fabricated BPF with cascade TSSIR.

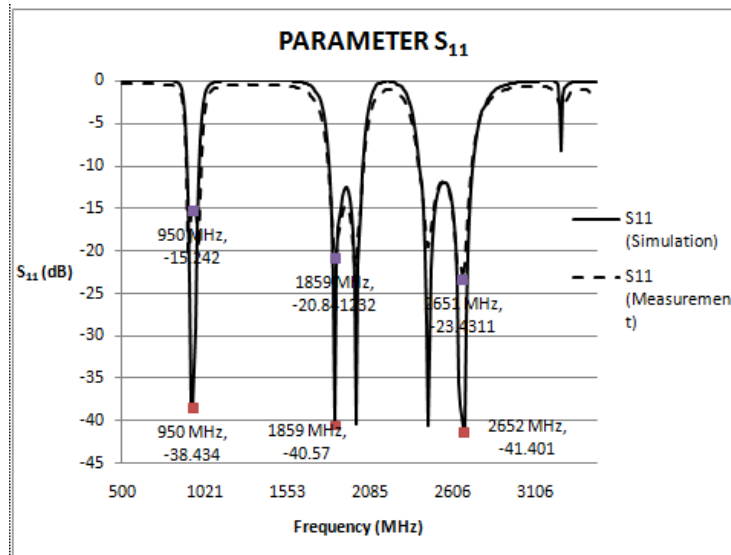


Figure 6 S_{11} results of the fabricated BPF using cascade TSSIR.

Figure 6 shows the S_{11} measurement results of the proposed BPF using cascade TSSIR. It can be seen from Figure 6 that the S_{11} performance of the fabricated BPF was in close agreement with the design requirement. This is due to the cascade construction being successful in getting transmission zero response at the third band. Therefore, the stopband response was improved. This indicates that the proposed BPF using cascade TSSIR can operate well at three frequencies simultaneously.

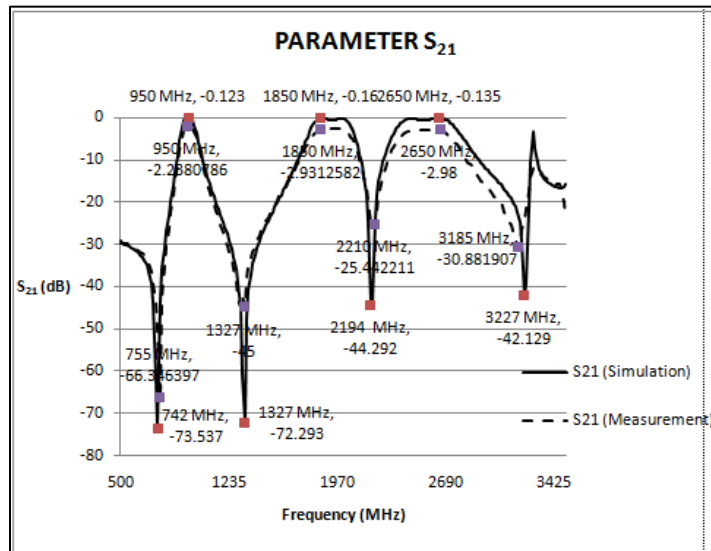


Figure 7 S₂₁ results of the fabricated BPF using cascade TSSIR.

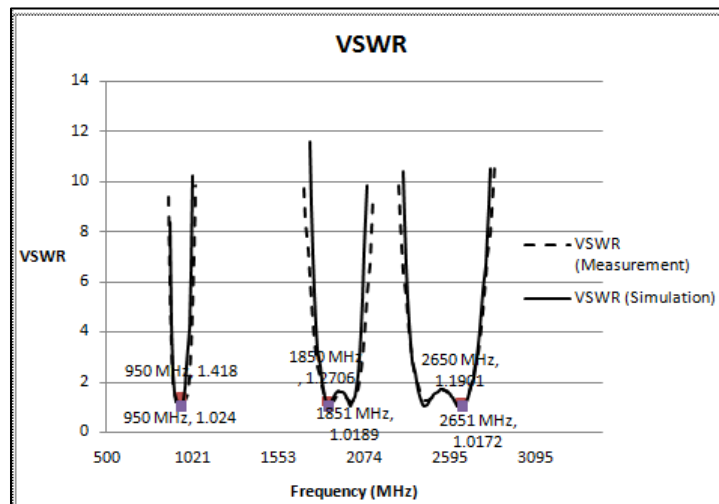


Figure 8 VSWR results of the fabricated BPF using cascade TSSIR.

Figure 7 shows a comparison of the S_{21} results of the simulated and the fabricated BPF using cascade TSSIR. It can be seen from Figure 7 that the S_{21} results of the fabricated BPF using TSSIR was in close agreement with the design requirement. This is because the proposed BPF using cascade TSSIR is successful in generating three passbands, hence it can transmit all power to the load and dissipates less power at BPF. It can be concluded that the proposed BPF using cascade TSSIR can be operated well at three frequencies simultaneously.

Figure 8 shows a comparison of the VSWR performance results of the simulated and the fabricated BPF. It can be seen from Figure 8 that the VSWR of both the simulated and the fabricated BPF satisfied the design specification, which was $VSWR < 2$. This is because the input and output impedances match with each other, so the proposed BPF using TSSIR was successful in passing all signals to the load at three frequencies simultaneously. It can be concluded that the proposed BPF using cascade TSSIR can be operated well at three frequencies simultaneously.

For comparison, the performance results of the simulated and the fabricated triple-band BPF using cascade TSSIR are shown in Table 4. It can be seen from Table 4 that performance results of the simulated and the fabricated triple-band BPF using cascade TSSIR were in close agreement with each other. This indicates that the proposed BPF using cascade TSSIR can operate well at three frequencies simultaneously.

Table 4 Comparison of performance results of simulated and fabricated triple-band BPF with cascade TSSIR.

Parameters	Simulated			Fabricated		
	950	1,850	2,650	950	1,850	2,650
f_c (MHz)	950	1,850	2,650	950	1,850	2,650
S_{21} (dB)	-0.12	-0.16	-0.14	-1.04	-1.73	-1.78
S_{11} (dB)	-38.43	-40.57	-41.40	-15.24	-20.84	-23.43
VSWR	1.02	1.16	1.03	1.42	1.27	1.19

The performances of the proposed triple-band BPF using TSSIR were better than the performances of the hairpin BPF using cascade TSSIR in Wibisono, *et al.* [10]. This is due to the construction of the proposed triple-band BPF using TSSIR, which was designed from two identical TSSIRs that are coupled at the third resonator and was successful in getting transmission zero response at the third band, so better stopband performance could be achieved. Also, the input/output port connected at the first resonator was successful in improving the BW of the proposed triple-band BPF using TSSIR.

5 Conclusion

A triple-band BPF using TSSIR that can operate at 900 MHz, 1,800 MHz and 2,600 MHz simultaneously was designed, fabricated and evaluated. The design and simulation of the proposed BPF were done using ADS. The proposed BPF using cascade TSSIR was fabricated on FR4 substrate with dielectric permittivity, substrate thickness and loss tangent at 4.3, 1.6 mm and 0.0017, respectively. It can be seen from the results that the performance results of both the simulated and the fabricated BPF using cascade TSSIR, characterized by return loss, insertion loss, VSWR and group delay, satisfied the performance standard and were in close agreement with each other. In addition to this, the results showed that the performances of the proposed BPF using cascade TSSIR were better than those of a hairpin BPF with TSSIR.

Acknowledgements

This research was supported by National Strategic Research Grant from Directorate Higher Education (DIKTI) Ministry of National Education of Republic Indonesia, 2012.

Reference

- [1] Chu, Q-X. & Lin, X-M., *Advanced Triple-Band Bandpass Filter Using Tri-Section SIR*, Electronics Letter, **44** (4), pp. 295-296, 2008.
- [2] Eroglu, A. & Smith. R., *Triple Band Bandpass Filter Design and Implementation Using SIRs*, Proc. of 2010 ACES Conference The 26th Annual Review of Progress in Applied Computational Electromagnetics, Tampere, Finland. pp. 862-865, 2010.
- [3] Moussa, R., Essaaidi, M., & Aghoutane, M., *Novel Compact Dual-and Tri-Band Filters Using Stepped Impedance Resonators*, Proc. of 2010 10th Mediterranean Microwave Symposium, North Cyprus, Turkey. pp. 403-406, 2010.
- [4] Chiou, Y-C., & Kuo, J-T., *Planar Multiband Bandpass Filter With Multimode Stepped Impedance Resonator*, PIER, **114**, pp. 129-144, 2011.
- [5] Lin, X.M., & Chu, Q. X., *Design of Triple-Band Bandpass Filter Using Tri-Section Stepped-Impedance Resonators*, Proc. of 2007 5th International Conference of Microwave and Millimeter Wave Technology (ICMMT 2007), **D1**(6), Gulin, China. pp. 1-3, 2007.
- [6] Lin, X.M., & Chu, Q.X., *A Novel Triple-Band Filter With Transmission Zeros Using Tri-Section SIRs*, Proc. of 2008 International Conference on Microwave and Millimeter Wave Technology (ICCMT 2008), Nanjing, China. pp. 1261-1263, 2007.

- [7] Zhang, H. & Chen, K.J., *A tri-Section Stepped Impedance Resonator for Cross-Coupled Bandpass Filter*, IEEE Microwave & Wireless Components Lett., **15**(6), pp. 401-403, 2005.
- [8] Packiaraj, D., Ramesh, M., & Kalghatgi, A.T., *Design of a Tri-Section Folded SIR Filter*, IEEE Microwave & Wireless Components Lett., **16**(5), pp. 317-319, 2006.
- [9] Makimoto, M. & Yamashita, S., *Bandpass Filters Using Parallel Coupled Stripline Stepped Impedance Resonators*. IEEE Transaction of Microwave Theory and Technique, IEEE Transactions on Microwave Theory and Techniques, **MTT-28** (12), pp. 1413-1417, 1980.
- [10] Wibisono, W. & Syafraditya, T., *Design of Triple-band Hairpin BPF Using Tri Section Stepped Impedance Resonators*, Proc. of 3rd Makassar Internasional Conference on Electrical Engineering and Informatics (MICEEI 2012), Makassar, Indonesia, pp. 58-62, 2012.
- [11] Hong, J-S. & Lancaster, M.J., *Microstrip Filters for RF/Microwave Applications*, John Wiley & Sons, Inc. New York, USA, 2001.